Explicit high-order noncanonical symplectic algorithms for ideal two-fluid systems

Jianyuan Xiao, Hong Qin, Philip J. Morrison, Jian Liu, Zhi Yu, Ruili Zhang, and Yang He

Citation: Physics of Plasmas **23**, 112107 (2016); doi: 10.1063/1.4967276
View online: http://dx.doi.org/10.1063/1.4967276
View Table of Contents: http://scitation.aip.org/content/aip/journal/pop/23/11?ver=pdfcov
Published by the AIP Publishing

Explicit high-order noncanonical symplectic algorithms for ideal two-fluid systems

Jianyuan Xiao,[1,2] Hong Qin,[1,3,a)] Philip J. Morrison,[4] Jian Liu,[1,2] Zhi Yu,[5] Ruili Zhang,[1,2] and Yang He[1,2]

[1]*School of Nuclear Science and Technology and Department of Modern Physics, University of Science and Technology of China, Hefei, Anhui 230026, China*
[2]*Key Laboratory of Geospace Environment, CAS, Hefei, Anhui 230026, China*
[3]*Plasma Physics Laboratory, Princeton University, Princeton, New Jersey 08543, USA*
[4]*Department of Physics and Institute for Fusion Studies, University of Texas at Austin, Austin, Texas 78741, USA*
[5]*Institute of Plasma Physics, Chinese Academy of Sciences, Hefei, Anhui 230031, China*

(Received 6 July 2016; accepted 21 October 2016; published online 9 November 2016)

An explicit high-order noncanonical symplectic algorithm for ideal two-fluid systems is developed. The fluid is discretized as particles in the Lagrangian description, while the electromagnetic fields and internal energy are treated as discrete differential form fields on a fixed mesh. With the assistance of Whitney interpolating forms [H. Whitney, *Geometric Integration Theory* (Princeton University Press, 1957); M. Desbrun *et al.*, *Discrete Differential Geometry* (Springer, 2008); J. Xiao *et al.*, Phys. Plasmas **22**, 112504 (2015)], this scheme preserves the gauge symmetry of the electromagnetic field, and the pressure field is naturally derived from the discrete internal energy. The whole system is solved using the Hamiltonian splitting method discovered by He *et al.* [Phys. Plasmas **22**, 124503 (2015)], which was been successfully adopted in constructing symplectic particle-in-cell schemes [J. Xiao *et al.*, Phys. Plasmas **22**, 112504 (2015)]. Because of its structure preserving and explicit nature, this algorithm is especially suitable for large-scale simulations for physics problems that are multi-scale and require long-term fidelity and accuracy. The algorithm is verified via two tests: studies of the dispersion relation of waves in a two-fluid plasma system and the oscillating two-stream instability. *Published by AIP Publishing.*
[http://dx.doi.org/10.1063/1.4967276]

I. INTRODUCTION

The ideal two-fluid model, a basic non-dissipative model of plasma physics, has been widely used to study fusion and astrophysical plasmas. In this model, the electrons and ions are treated as ideal fluids separately, with coupling to the electromagnetic fields through the charge and current carried by them. Although this system is easily generalized to any number of different charged species, the terminology "two-fluid" will be used here in lieu of "multi-fluid," as is typically done. Because the ideal two-fluid system has noncanonical Hamiltonian form,[5,6] as was shown in Ref. 7, its dynamics preserves the geometric structure and there is no dissipation of invariants such as the total energy and momentum in the system. Conventional numerical algorithms for the ideal two-fluid system generally do not preserve the geometric structure and thus the truncation error can accumulate coherently over simulation time-steps. This is a serious drawback when solving most electron-ion systems whose behaviors are naturally multi-scale. For example, the ion cyclotron period is thousands of times longer than that of the electron.

Symplectic methods, discovered in the 1980s,[8–23] have proven to be efficient for solving finite-dimensional canonical Hamiltonian systems. Such methods preserve the symplectic geometric structure (2-form) associated with the original canonical Hamiltonian system, and the numerical error of all invariants can be globally bounded by small values throughout simulations.[24] In plasma physics, accelerator physics, and fluid dynamics, many of the finite-dimensional Hamiltonian systems and most of the infinite-dimensional Hamiltonian systems are noncanonical; for example, this is the case for guiding center dynamics,[25–27] the Euler fluid and magnetohydrodynamics (MHD) equations,[28] the Vlasov-Maxwell and Vlasov-Poisson systems,[5,6,29–31] and drift and gyrokinetic theories.[32–36] The development of geometric algorithms for these systems can be challenging. However, recently significant advances have been achieved in the development of structure preserving geometric algorithms for charged particle dynamics,[37–50] the Vlasov-Maxwell systems,[3,4,51–61] compressible ideal MHD,[62,63] and incompressible fluids.[64,65] All of these methods have demonstrated unparalleled long-term numerical accuracy and fidelity compared with conventional methods. As a side note, we point out that for infinite-dimensional Hamiltonian systems, an alternative viewpoint is to treat them as multi-symplectic systems,[66,67] and corresponding multi-symplectic algorithms[68–74] have also been developed.

In the present work, an explicit, high-order, noncanonical symplectic algorithm for integrating the compressible

[a)]Author to whom correspondence should be addressed. Electronic mail: hongqin@ustc.edu.cn

ideal two-fluid system is developed. We discretize the fluid as particles in the Lagrangian description, which naturally guarantees conservation of the density. The electromagnetic fields and internal energy are discretized over a cubic mesh by using the theory of discrete exterior calculus (DEC).[75] High-order Whitney interpolating forms[3] are used to ensure the gauge symmetry of Maxwell's equations. The discrete Poisson bracket for the ideal two-fluid system is obtained by a similar technique that is used in obtaining the discrete Vlasov-Maxwell bracket,[3] and the final numerical scheme is constructed by the powerful Hamiltonian split method.[3,4,47] We note that for the existing structure preserving method for the compressible fluid,[62] all fields are discretized over a moving mesh, which does not apply to cases where the mesh deforms significantly during the evolution, such as in a rotating fluid. This difficulty is overcome by using a fixed mesh rather than a moving one for discretizing the electromagnetic and internal energy fields in our method. The conservation of symplectic structure guarantees that the numerical errors of all invariants such as the total energy and momentum are bounded within a small value during the simulations.[24] Therefore, this method is most suitable for solving long-term multi-scale problems.

The paper is organized as follows. In Sec. II, the Hamiltonian theory of the ideal two-fluid system is reviewed and the geometric structure preserving method is developed. Two numerical examples, the dispersion relation of waves in an ideal two-fluid system and the oscillating two-stream instability, are given in Sec. III. Finally, in Sec. IV we conclude.

II. STRUCTURE PRESERVING DISCRETIZATION FOR IDEAL TWO-FLUID SYSTEMS

The starting point of our development is the Lagrangian of the ideal two-fluid system, written in terms of Lagrangian variables, which is quite similar to the Lagrangian for the Vlasov-Maxwell system except for the addition of internal energy terms (see, e.g., Ref. 76). This Lagrangian is given as follows:

$$\mathcal{L}=\sum_s\int \mathrm{d}\mathbf{x}_0\left(\frac{1}{2}n_{s0}(\mathbf{x}_0)m_s|\dot{\mathbf{x}}_s|^2+q_sn_{s0}(\mathbf{x}_0)\dot{\mathbf{x}}_s\cdot\mathbf{A}(\mathbf{x}_s)\right.$$
$$\left.-U_{ms}\left(\frac{n_{s0}(\mathbf{x}_0)m_s}{\mathcal{J}(\mathbf{x}_s)}\right)\right)+\frac{1}{2}\int \mathrm{d}^3\mathbf{x}\left(|\dot{\mathbf{A}}(\mathbf{x})|^2-|\nabla\times\mathbf{A}(\mathbf{x})|^2\right), \tag{1}$$

where m_s, q_s, and n_{s0} are the mass, charge, and initial number density distribution of species s, respectively, $\mathbf{x}_s$ and $\dot{\mathbf{x}}_s$ are current position and velocity of fluid elements for species s labeled by $\mathbf{x}_0$, which we take to be the initial value of $\mathbf{x}_s$ in the configuration space, $\mathcal{J}(\mathbf{x}_s)$ is the Jacobian of the coordinate transformation from the initial value $\mathbf{x}_0$–$\mathbf{x}_s$, U_{ms} is the internal energy per unit mass for species s, and $\mathbf{A}$ is the electromagnetic vector potential. In the arguments of the fields $\mathbf{x}_s$ and $\mathbf{A}$ we suppress the time variable. In this Lagrangian, we have ignored the entropy term in the internal energy, assuming barotropic fluids, and adopted the temporal gauge with $\phi=0$. The permittivity and permeability are set to unity for simplicity.

Evolution equations are obtained upon variation of the action S as in Hamilton's principle

$$\delta S[\mathbf{x}_s,\mathbf{A}]=\delta\int \mathrm{d}t\,\mathcal{L}=0, \tag{2}$$

giving rise the equations of motion via

$$\frac{\delta S}{\delta\mathbf{x}_s}=0\quad\text{and}\quad\frac{\delta S}{\delta\mathbf{A}}=0, \tag{3}$$

which yield

$$m_s\ddot{\mathbf{x}}_s(\mathbf{x}_0)=q_s\left(\dot{\mathbf{x}}_s\times\mathbf{B}(\mathbf{x}_s)+\mathbf{E}(\mathbf{x}_s)\right)$$
$$-\frac{1}{n_{s0}(\mathbf{x}_0)}\frac{\partial U_{ms}\left(\frac{n_{s0}(\mathbf{x}_0)m_s}{\mathcal{J}(\mathbf{x}_s)}\right)}{\partial\mathbf{x}_s}, \tag{4}$$

$$\dot{\mathbf{E}}(\mathbf{x})=\nabla\times\mathbf{B}(\mathbf{x})-\sum_s\int \mathrm{d}\mathbf{x}_0\,q_sn_{s0}(\mathbf{x}_0)\dot{\mathbf{x}}_s\delta(\mathbf{x}-\mathbf{x}_s), \tag{5}$$

where $\mathbf{E}=-\dot{\mathbf{A}}$ and $\mathbf{B}=\nabla\times\mathbf{A}$ are the electromagnetic fields. These equations are exactly the ideal two-fluid equations in the Lagrangian variable description.

Now we discretize the Lagrangian using a method very similar to that for the discretization of the Vlasov-Maxwell system in Ref. 3. The electromagnetic fields and internal energy are sampled over a cubic mesh, while the fluid is discretized into finite-sized smooth particles[3,53,77] moving between mesh grids. Modeling fluids using a set of Lagrangian particles is also the key idea of the smoothed-particle-hydrodynamics (SPH) method.[77–79] However, the difference is that our internal energy fields are calculated on fixed mesh grids. Therefore, the method developed in the present study more closely resembles the structure-preserving symplectic particle-in-cell (PIC) method of Ref. 3. The resulting discrete Lagrangian is

$$\mathcal{L}_d=\sum_{s,p}\left(\frac{1}{2}m_sn_{0,sp}|\dot{\mathbf{x}}_{sp}|^2+q_sn_{0,sp}\dot{\mathbf{x}}_{sp}\cdot\sum_J\mathbf{A}_JW_{\sigma_{1J}}(\mathbf{x}_{sp})\right)$$
$$-\sum_{s,I}U_s(\rho_{sI})+\frac{1}{2}\sum_J\left(|\dot{\mathbf{A}}_J|^2-|\mathrm{curl_d}\mathbf{A}_J|^2\right), \tag{6}$$

where

$$\rho_{sI}=\sum_p m_sn_{0,sp}W_{\sigma_{0I}}(\mathbf{x}_{sp}). \tag{7}$$

Here, the subscript sp denotes the p-th particle of species s, $W_{\sigma_{0I}}$ and $W_{\sigma_{1J}}$ are Whitney interpolating maps for discrete 0-forms and 1-forms,[1–3,75] U_s is discrete internal energy per unit volume for species s, $\mathrm{curl_d}$ is the discrete curl operator that is defined in Eq. (15), I, J, K are indices for the discrete 0-form, 1-form, 2-form, respectively. To simplify the notation, the grid size Δx has been set to unity. The Whitney maps are defined as follows:

$$\sum_{i,j,k} W_{\sigma_{0,i,j,k}}(\mathbf{x})\phi_{i,j,k} \equiv \sum_{i,j,k} \phi_{i,j,k} W_1(x)W_1(y)W_1(z),$$

$$\sum_{i,j,k} W_{\sigma_{1,i,j,k}}(\mathbf{x})\mathbf{A}_{i,j,k} \equiv \sum_{i,j,k} \begin{bmatrix} A_{xi,j,k}W_1^{(2)}(x-i)W_1(y-j)W_1(z-k) \\ A_{yi,j,k}W_1(x-i)W_1^{(2)}(y-j)W_1(z-k) \\ A_{zi,j,k}W_1(x-i)W_1(y-j)W_1^{(2)}(z-k) \end{bmatrix}^T,$$

$$\sum_{i,j,k} W_{\sigma_{2,i,j,k}}(\mathbf{x})\mathbf{B}_{i,j,k} \equiv \sum_{i,j,k} \begin{bmatrix} B_{xi,j,k}W_1(x-i)W_1^{(2)}(y-j)W_1^{(2)}(z-k) \\ B_{yi,j,k}W_1^{(2)}(x-i)W_1(y-j)W_1^{(2)}(z-k) \\ B_{zi,j,k}W_1^{(2)}(x-i)W_1^{(2)}(y-j)W_1(z-k) \end{bmatrix}^T,$$

$$\sum_{i,j,k} W_{\sigma_{3,i,j,k}}(\mathbf{x})\rho_{i,j,k} \equiv \sum_{i,j,k} \rho_{i,j,k} W_1^{(2)}(x-i)W_1^{(2)}(y-j)W_1^{(2)}(z-k),$$

$$W_1^{(2)}(x) = -\begin{cases} W_1'(x) + W_1'(x+1) + W_1'(x+2)\,, -1 \le x < 2, \\ 0\,, \text{otherwise}\,. \end{cases}$$

where the one-dimensional interpolation function W_1 is chosen in this paper to be

$$W_1(x) = \begin{cases} 0, & x \le -2, \\ -\frac{x^6}{48} - \frac{x^5}{8} - \frac{5x^4}{16} - \frac{5x^3}{12} + x + 1, & -2 < x \le -1, \\ \frac{x^6}{48} - \frac{x^5}{8} - \frac{5x^4}{16} - \frac{5x^3}{12} - \frac{5x^2}{8} + \frac{7}{12}, & -1 < x \le 0, \\ \frac{x^6}{48} + \frac{x^5}{8} - \frac{5x^4}{16} + \frac{5x^3}{12} - \frac{5x^2}{8} + \frac{7}{12}, & 0 < x \le 1, \\ -\frac{x^6}{48} + \frac{x^5}{8} - \frac{5x^4}{16} + \frac{5x^3}{12} - x + 1, & 1 < x \le 2, \\ 0, & 2 < x\,. \end{cases} \tag{8}$$

The equations of motion arising from the action with Lagrangian $\mathcal{L}_d$ of (6) are the following:

$$m_s n_{0,sp}\ddot{\mathbf{x}}_{sp} = q_s n_{0,sp}\left(\dot{\mathbf{x}}_{sp} \times \left(\nabla \times \sum_J \mathbf{A}_J W_{\sigma_{1J}}(\mathbf{x}_{sp})\right) - \dot{\mathbf{A}}_J W_{\sigma_{1J}}(\mathbf{x}_{sp})\right) - \sum_I U_s'(\rho_{sI}) m_s n_{0,sp} \nabla W_{\sigma_{0I}}(\mathbf{x}_{sp}), \tag{9}$$

$$\ddot{\mathbf{A}}_J = -\mathrm{curl}_\mathrm{d}^T \mathrm{curl}_\mathrm{d} \mathbf{A}_J + \sum_{s,p} q_s n_{0,sp} \mathbf{x}_{sp} W_{\sigma_{1J}}(\mathbf{x}_{sp}). \tag{10}$$

Next, we introduce two discrete fields $\mathbf{E}_J = -\dot{\mathbf{A}}_J$ and $\mathbf{B}_K = \sum_J \mathrm{curl}_{\mathrm{d}\,KJ}\mathbf{A}_J$, which are discrete electromagnetic fields. We will make use of the following properties of the interpolating forms[1,3,75]

$$\nabla \sum_I W_{\sigma_{0I}}(\mathbf{x})\phi_I = \sum_{I,J} W_{\sigma_{1J}}(\mathbf{x})\nabla_{\mathrm{d}JI}\phi_I, \tag{11}$$

$$\nabla \times \sum_J W_{\sigma_{1J}}(\mathbf{x})\mathbf{A}_J = \sum_{J,K} W_{\sigma_{2K}}(\mathbf{x})\mathrm{curl}_{\mathrm{d}KJ}\mathbf{A}_J, \tag{12}$$

$$\nabla \cdot \sum_K W_{\sigma_{2K}}(\mathbf{x})\mathbf{B}_K = \sum_{K,L} W_{\sigma_{3L}}(\mathbf{x})\mathrm{div}_{\mathrm{d}LK}\mathbf{B}_K, \tag{13}$$

$$(\nabla_\mathrm{d}\phi)_{i,j,k} = [\phi_{i+1,j,k} - \phi_{i,j,k}, \phi_{i,j+1,k} - \phi_{i,j,k}, \phi_{i,j,k+1} - \phi_{i,j,k}]. \tag{14}$$

$$(\mathrm{curl}_\mathrm{d}\mathbf{A})_{i,j,k} = \begin{bmatrix} (A_{zi,j+1,k} - A_{zi,j,k}) - (A_{yi,j,k+1} - A_{yi,j,k}) \\ (A_{xi,j,k+1} - A_{xi,j,k}) - (A_{zi+1,j,k} - A_{zi,j,k}) \\ (A_{yi+1,j,k} - A_{yi,j,k}) - (A_{xi,j+1,k} - A_{xi,j,k}) \end{bmatrix}^T, \tag{15}$$

$$(\mathrm{div}_\mathrm{d}\mathbf{B})_{i,j,k} = (B_{xi+1,j,k} - B_{xi,j,k}) + (B_{yi,j+1,k} - B_{yi,j,k}) + (B_{zi,j,k+1} - B_{zi,j,k}), \tag{16}$$

which hold for any ϕ_I, $\mathbf{A}_J$, and $\mathbf{B}_K$. With these identities, Eqs. (9) and (10) can be expressed as

$$m_s n_{0,sp}\ddot{\mathbf{x}}_{sp} = q_s n_{0,sp}\left(\dot{\mathbf{x}}_{sp} \times \sum_K \mathbf{B}_K W_{\sigma_{2K}}(\mathbf{x}_{sp}) + \mathbf{E}_J W_{\sigma_{1J}}(\mathbf{x}_{sp})\right) - \sum_I U_i'(\rho_{sI}) m_s n_{0,sp} \nabla W_{\sigma_{0I}}(\mathbf{x}_{sp})\,, \tag{17}$$

$$\dot{\mathbf{E}}_J = \sum_K \mathrm{curl}^T_{\mathrm{d}JK}\mathbf{B}_K - \sum_{s,p} q_s n_{0,sp}\dot{\mathbf{x}}_{sp} W_{\sigma_{1J}}(\mathbf{x}_{sp}), \tag{18}$$

$$\dot{\mathbf{B}}_K = -\sum_J \mathrm{curl}_{\mathrm{d}KJ}\mathbf{E}_J. \tag{19}$$

The continuity equations for the densities are automatically satisfied, as can be shown by directly calculating the time derivative of ρ_{sI}

$$\dot{\rho}_{sI} = \sum_p m_s n_{0,sp}\dot{\mathbf{x}}_{sp}\cdot\nabla W_{\sigma_{0I}}(\mathbf{x}_{sp}), \tag{20}$$

$$= \sum_p m_s n_{0,sp}\dot{\mathbf{x}}_{sp}\cdot\sum_J W_{\sigma_{1J}}(\mathbf{x}_{sp})\nabla_{\mathrm{d}JI}, \tag{21}$$

$$= \sum_J \nabla_{\mathrm{d}JI}\sum_p m_s n_{0,sp}\dot{\mathbf{x}}_{sp}\cdot W_{\sigma_{1J}}(\mathbf{x}_{sp}), \tag{22}$$

$$= \sum_J \nabla_{\mathrm{d}JI}\mathbf{M}_{sJ}, \tag{23}$$

where $\mathbf{M}_{sJ}$ can be viewed as the discrete momentum density over mesh grids, and $\sum_J\nabla_{\mathrm{d}JI}$ is a discrete version of $-\nabla\cdot$. So, Eq. (23) is essentially a kind of discrete continuity equation. Using a similar technique, we can also prove the discrete charge conservation property

$$\sum_s \frac{q_s}{m_s}\dot{\rho}_{sI} = \sum_{s,J}\nabla_{\mathrm{d}JI}\frac{q_s}{m_s}\mathbf{M}_{sJ}. \tag{24}$$

With this property and using Eq. (18) we can see that the discrete Gauss's law

$$\sum_J \nabla_{\mathrm{d}JI}\mathbf{E}_J + \sum_{s,p}\frac{q_s}{m_s}\rho_{sI} = 0, \tag{25}$$

is satisfied for all times if it is satisfied initially. The charge conservation has close relation to the gauge invariance. Squire *et al.*[52] first constructed a discrete system for PIC simulations with gauge invariance and showed that gauge invariance guarantees the charge conservation for the discrete system. Recently, Burby and Tronci[80] found that in the field theory for hybrid models, the gauge invariance of the theory is necessary and sufficient to ensure charge conservation for the system.

To construct the geometric structure preserving algorithm, the Hamiltonian theory for the discretized system is considered. Note that the only difference between the two-fluid Lagrangian and the Vlasov-Maxwell Lagrangian is the internal energy term, which can be written as a function of $\mathbf{x}_{sp}$. Thus, the discrete Poisson structure of the ideal two-fluid system can be chosen to be the same as that for the Vlasov-Maxwell system,[3] which is

$$\begin{aligned}\{F,G\} =& \sum_J\left(\frac{\partial F}{\partial \mathbf{E}_J}\cdot\sum_K\frac{\partial G}{\partial \mathbf{B}_K}\mathrm{curl}_{\mathrm{d}KJ} - \sum_K\frac{\partial F}{\partial \mathbf{B}_K}\mathrm{curl}_{\mathrm{d}KJ}\cdot\frac{\partial G}{\partial \mathbf{E}_J}\right)\\ &+\sum_{s,p}\frac{1}{m_s n_{0,sp}}\left(\frac{\partial F}{\partial \mathbf{x}_{sp}}\cdot\frac{\partial G}{\partial \dot{\mathbf{x}}_{sp}} - \frac{\partial F}{\partial \dot{\mathbf{x}}_{sp}}\cdot\frac{\partial G}{\partial \mathbf{x}_{sp}}\right) + \sum_{s,p}\frac{q_s}{m_s}\\ &\times\left(\frac{\partial F}{\partial \dot{\mathbf{x}}_{sp}}\cdot\sum_J W_{\sigma_{1J}}(\mathbf{x}_{sp})\frac{\partial G}{\partial \mathbf{E}_J} - \frac{\partial G}{\partial \dot{\mathbf{x}}_{sp}}\cdot\sum_J W_{\sigma_{1J}}(\mathbf{x}_{sp})\frac{\partial F}{\partial \mathbf{E}_J}\right)\\ &-\sum_{s,p}\frac{q_s}{m_s^2 n_{0,sp}}\frac{\partial F}{\partial \dot{\mathbf{x}}_{sp}}\cdot\left[\sum_K W_{\sigma_{2K}}(\mathbf{x}_{sp})\mathbf{B}_K\right]\times\frac{\partial G}{\partial \dot{\mathbf{x}}_{sp}}.\end{aligned}$$

And the two-fluid Hamiltonian is

$$H = \frac{1}{2}\left(\sum_J \mathbf{E}_J^2 + \sum_K \mathbf{B}_K^2 + \sum_{s,p} m_s n_{0,sp}|\dot{\mathbf{x}}_{sp}|^2\right) + \sum_{sI} U_s(\rho_{sI}). \tag{26}$$

It is straightforward to check that the following Hamiltonian equations are identical to Eqs. (17)–(19)

$$\dot{\mathbf{x}}_{sp} = \{\mathbf{x}_{sp}, H\}, \tag{27}$$

$$\ddot{\mathbf{x}}_{sp} = \{\dot{\mathbf{x}}_{sp}, H\}, \tag{28}$$

$$\dot{\mathbf{E}}_J = \{\mathbf{E}_J, H\}, \tag{29}$$

$$\dot{\mathbf{B}}_K = \{\mathbf{B}_K, H\}. \tag{30}$$

Now the discrete algorithm can be developed. Using a Hamiltonian splitting technique similar to that in Refs. 3 and 4, H can be split into 6 parts

$$H = H_E + H_B + H_x + H_y + H_z + H_U, \tag{31}$$

where

$$H_E = \frac{1}{2}\sum_J \mathbf{E}_J^2, \tag{32}$$

$$H_B = \frac{1}{2}\sum_K \mathbf{B}_K^2, \tag{33}$$

$$H_r = \frac{1}{2}\sum_{s,p} m_s n_{0,sp}\dot{r}_{sp}^2, \quad \text{for } r\in\{x,y,z\}, \tag{34}$$

$$H_U = \sum_{s,I} U_s(\rho_{sI}). \tag{35}$$

It turns out that the exact solutions for all sub-systems can be found and computed explicitly. The exact solutions for H_E, H_B, H_x, H_y, and H_z have been derived in Ref. 3. They are

$$\Theta_E:\begin{cases}\mathbf{E}_J(t+\Delta t) = \mathbf{E}_J(t),\\ \mathbf{B}_K(t+\Delta t) = \mathbf{B}_K(t) - \Delta t\sum_J \mathrm{curl}_{\mathrm{d}KJ}\mathbf{E}_J(t),\\ \mathbf{x}_{sp}(t+\Delta t) = \mathbf{x}_{sp}(t),\\ \dot{\mathbf{x}}_{sp}(t+\Delta t) = \dot{\mathbf{x}}_{sp}(t) + \frac{q_s}{m_s}\Delta t\sum_J W_{\sigma_{1J}}(\mathbf{x}_{sp}(t))\mathbf{E}_J(t),\end{cases} \tag{36}$$

$$\Theta_B:\begin{cases}\mathbf{E}_J(t+\Delta t) = \mathbf{E}_J(t) + \Delta t\sum_K \mathrm{curl}_{\mathrm{d}KJ}\mathbf{B}_K(t),\\ \mathbf{B}_K(t+\Delta t) = \mathbf{B}_K(t),\\ \mathbf{x}_{sp}(t+\Delta t) = \mathbf{x}_{sp}(t),\\ \dot{\mathbf{x}}_{sp}(t+\Delta t) = \dot{\mathbf{x}}_{sp}(t),\end{cases} \tag{37}$$

$$\Theta_x:\begin{cases}\mathbf{E}_J(t+\Delta t)=\mathbf{E}_J(t)-\int_0^{\Delta t}dt'\sum_{s,p}q_s n_{0,sp}\dot{x}_{sp}(t)\mathbf{e}_x W_{\sigma_{1J}}\left(\mathbf{x}_{sp}(t)+\dot{x}_{sp}(t)t'\mathbf{e}_x\right)\\ \mathbf{B}_K(t+\Delta t)=\mathbf{B}_K(t),\\ \mathbf{x}_{sp}(t+\Delta t)=\mathbf{x}_{sp}(t)+\Delta t\dot{x}_{sp}(t)\mathbf{e}_x,\\ \dot{\mathbf{x}}_{sp}(t+\Delta t)=\dot{\mathbf{x}}_{sp}(t)+\frac{q_s}{m_s}\dot{x}_{sp}(t)\mathbf{e}_x\times\int_0^{\Delta t}dt'\sum_K W_{\sigma_{2K}}\left(\mathbf{x}_{sp}(t)+\dot{x}_{sp}(t)t'\mathbf{e}_x\right)\mathbf{B}_K(t).\end{cases}\tag{38}$$

The solutions Θ_y and Θ_z are similar to Θ_x. For H_U, the exact evolution equations are

$$\dot{\mathbf{E}}_J=\{\mathbf{E}_J,H_U\}=0,\tag{39}$$

$$\dot{\mathbf{B}}_K=\{\mathbf{B}_K,H_U\}=0,\tag{40}$$

$$\dot{\mathbf{x}}_{sp}=\{\mathbf{x}_{sp},H_U\}=0,\tag{41}$$

$$\ddot{\mathbf{x}}_{sp}=\{\dot{\mathbf{x}}_{sp},H_U\}=-\sum_I {U_s}'(\rho_{sI})\nabla W_{\sigma_{0I}}(\mathbf{x}_{sI}).\tag{42}$$

Using the property Eq. (11) of the Whitney interpolating forms, the exact solution can be written as

$$\Theta_U:\begin{cases}\mathbf{E}_J(t+\Delta t)=\mathbf{E}_J(t),\\ \mathbf{B}_K(t+\Delta t)=\mathbf{B}_K(t),\\ \mathbf{x}_{sp}(t+\Delta t)=\mathbf{x}_{sp}(t),\\ \dot{\mathbf{x}}_{sp}(t+\Delta t)=\dot{\mathbf{x}}_{sp}(t)-\Delta t\sum_{I,J}\nabla_{\mathrm{d}JI}U_s'(\rho_{sI})W_{\sigma_{1J}}(\mathbf{x}_{sp}).\end{cases}\tag{43}$$

Here, Θ_U can be interpreted as a discrete version of the continuous Newton's second law

$$\ddot{\mathbf{x}}_s=-\nabla_{\mathbf{x}_s}U_s'\left(\frac{m_s n_{s0}}{\mathcal{J}_s}\right).\tag{44}$$

At first look, it seems different from Newton's law in the Lagrangian form derived in Ref. 6, i.e.

$$\ddot{\mathbf{x}}=-\mathcal{J}\nabla\left(\frac{\rho_0}{\mathcal{J}^2}U_m'\left(\frac{\rho_0}{\mathcal{J}}\right)\right).\tag{45}$$

This is because the U_m in Eq. (45) is defined as the internal energy per mass. Upon letting $\rho_0=m_s n_{s0}$, the relation between U_{ms} and U_s is

$$U_s\left(\frac{m_s n_{s0}}{\mathcal{J}}\right)=\frac{m_s n_{s0}}{\mathcal{J}}U_{ms}\left(\frac{m_s n_{s0}}{\mathcal{J}}\right).\tag{46}$$

Consequently

$$\begin{aligned}&-\nabla U_s'\left(\frac{m_s n_{s0}}{J}\right)\\&=-\nabla\left(U_{ms}\left(\frac{m_s n_{s0}}{J}\right)+\frac{m_s n_{s0}}{\mathcal{J}}U_{ms}'\left(\frac{m_s n_{s0}}{J}\right)\right)\\&=\nabla\mathcal{J}\frac{m_s n_{s0}}{\mathcal{J}^2}U_{ms}'\left(\frac{m_s n_{s0}}{J}\right)-\nabla\left(\frac{m_s n_{s0}}{\mathcal{J}}U_{ms}'\left(\frac{m_s n_{s0}}{J}\right)\right)\\&=-\mathcal{J}\nabla\left(\frac{m_s n_{s0}}{\mathcal{J}^2}U_{ms}'\left(\frac{m_s n_{s0}}{J}\right)\right),\end{aligned}$$

which is identical to the pressure term in the right hand side of Eq. (45). Therefore, the pressure for the species s can be defined to be[6]

$$\begin{aligned}P_s&=\frac{m_s^2 n_{s0}^2}{\mathcal{J}^2}U_{ms}'\left(\frac{m_s n_{s0}}{J}\right)\\&=\frac{m_s n_{s0}}{\mathcal{J}}U_s'\left(\frac{m_s n_{s0}}{J}\right)-U_s\left(\frac{m_s n_{s0}}{J}\right)\\&=\rho_s U_s'(\rho_s)-U_s(\rho_s).\end{aligned}$$

The final geometric structure-preserving scheme can be constructed from these exact solutions. For example, a first-order scheme can be chosen as

$$\Theta_1(\Delta t)=\Theta_E(\Delta t)\Theta_B(\Delta t)\Theta_x(\Delta t)\Theta_y(\Delta t)\Theta_z(\Delta t)\Theta_U(\Delta t),\tag{47}$$

and a second-order scheme can be constructed as

$$\begin{aligned}\Theta_2(\Delta t)=&\Theta_x(\Delta t/2)\Theta_y(\Delta t/2)\Theta_z(\Delta t/2)\Theta_B(\Delta t/2)\\&\times\Theta_U(\Delta/2)\Theta_E(\Delta t)\Theta_U(\Delta t/2)\Theta_B(\Delta t/2)\\&\times\Theta_z(\Delta t/2)\Theta_y(\Delta t/2)\Theta_x(\Delta t/2).\end{aligned}\tag{48}$$

The $2(l+1)$ th-order scheme can be derived from the $2l$th-order scheme by using

$$\Theta_{2(l+1)}(\Delta t)=\Theta_{2l}(\alpha_l\Delta t)\Theta_{2l}(\beta_l\Delta t)\Theta_{2l}(\alpha_l\Delta t),\tag{49}$$

$$\alpha_l=1/(2-2^{1/(2l+1)}),\tag{50}$$

$$\beta_l=1-2\alpha_l.\tag{51}$$

III. NUMERICAL EXAMPLES

To verify the practicability of our explicit high-order noncanonical symplectic algorithm for ideal two-fluid systems, we apply it to two physics problems. In the first problem, we examine the dispersion relation of an electron-deuterium plasma, while the second concerns the oscillation two-stream instability.

For the electron-deuterium plasma, parameters of the unperturbed uniform plasma are chosen as follows:

$$n_{i_0}=n_{e_0}=4.0\times10^{19}\,\mathrm{m}^{-3},\tag{52}$$

$$\rho_{e_0}=n_{e_0}m_e,\tag{53}$$

$$\rho_{i_0}=n_{i_0}m_i,\tag{54}$$

$$m_i=3671m_e=3.344\times10^{-27}\,\mathrm{kg},\tag{55}$$

$$q_i = -q_e = 1.602 \times 10^{-19}\text{C}, \tag{56}$$

$$U_e(\rho_e) = U_{e_0}\frac{3}{2}\left(\frac{\rho_e}{\rho_{e_0}}\right)^{5/3}, \tag{57}$$

$$U_i(\rho_i) = U_{i_0}\frac{3}{2}\left(\frac{\rho_i}{\rho_{i_0}}\right)^{5/3}, \tag{58}$$

$$\mathbf{B}_0 = (3.17\mathbf{e}_z + 1.13\mathbf{e}_y)\text{T}, \tag{59}$$

where $U_{i_0} = U_{e_0} = m_e n_e v_{Te}^2/2, v_{Te} = 0.04472\text{c}$, c is the speed of light in the vacuum, $\mathbf{B}_0$ is the constant external magnetic field. This plasma supports both electron waves and ion waves, and their frequencies are very different since the deuterium ion is much heavier than the electron. The simulation is carried out in a $1 \times 1 \times 1536$ mesh, and the periodical boundary condition is adopted in all x, y, and z directions. The grid size is chosen to be $\Delta x = 2 \times 10^{-4}$ m and the time step is set to $\Delta t = \Delta x/(2\text{c})$. The simulation is initialized with stationary fluid particles being equally spaced with 4 particles per grid cell.

To numerically obtain the dispersion relation, the simulation is carried out with a small random perturbation. The space-time dependence of one field component is transformed into $\omega - k$ space, and a contour plot of the field component in the $\omega - k$ space is used to make correspondence with the linear dispersion relation of the discrete system. In Fig. 1, such a contour plot is compared with the theoretical dispersion relation in both high frequency and low frequency ranges. We can see that the dispersion relation obtained by our geometric two-fluid algorithm agrees very well with the theory over the frequency range of the simulation. As expected, the total energy of the system is bounded to be within an interval of its initial value of for all simulation time-steps, which is plotted in Fig. 2.

The second example is the well-known oscillating two-stream instability.[81,82] We consider the case of an unmagnetized cold two-fluid model and compare with stability condition that was previously studied in Ref. 83. We simulate an electron-positron plasma, with system parameters given as follows:

$$n_{e0} = n_{i0} = 4.0 \times 10^{15}\,\text{m}^{-3}, \tag{60}$$

$$m_i = m_e = 9.1 \times 10^{-31}\,\text{kg}, \tag{61}$$

$$\mathbf{B}_0 = 0, \tag{62}$$

with the relative drift velocity between electrons and positrons chosen to be $\mathbf{v}_d/2 = \mathbf{v}_{e0} = -\mathbf{v}_{i0} = \mathbf{e}_z 0.041\text{c}$. The simulation domain is a $1 \times 1 \times 256$ mesh. Initial perturbations with two different wave numbers, $k_z = \pi/128$ and $k_z = \pi/32$, are tested. According to the theoretical prediction of Ref. 83, the mode with $k_z = \pi/32$ is stable while that with $k_z = \pi/128$ is unstable. Both of these predictions are confirmed by the

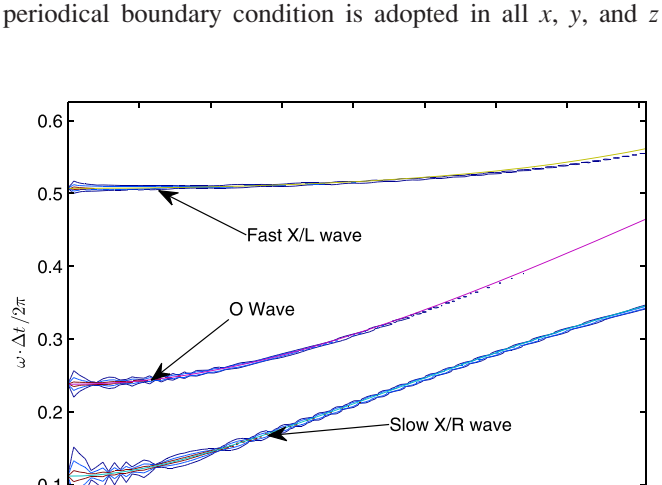

(a) High frequency region.

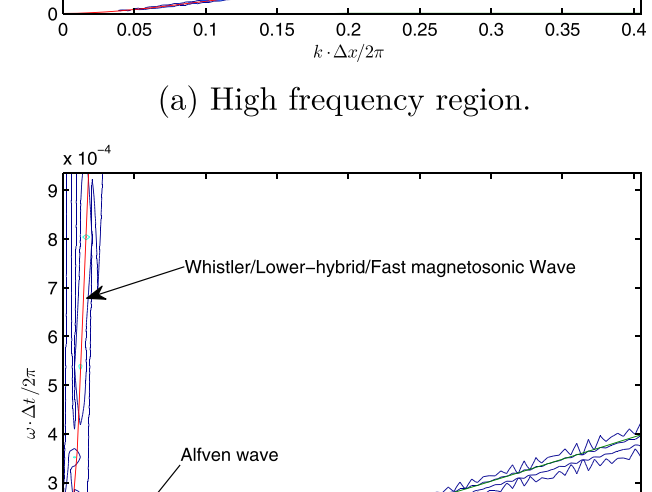

(b) Low frequency region.

FIG. 1. The dispersion relation of an electron-deuterium two-fluid plasma plotted against simulation results. The high frequency region is shown in (a) and the low frequency region in (b), with solid lines being theoretical dispersion relation.

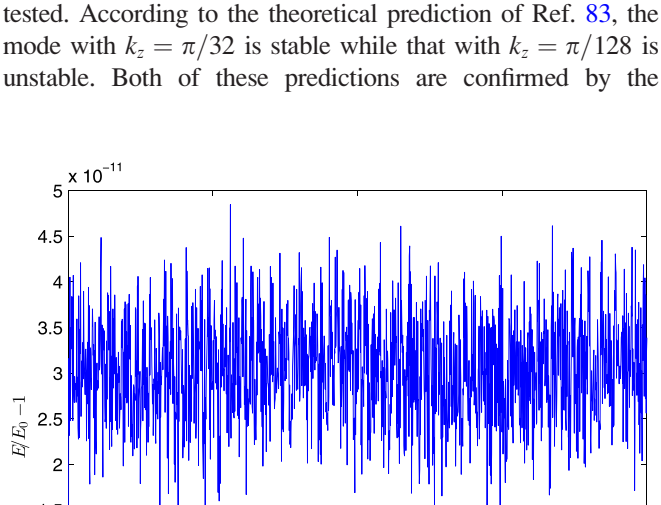

FIG. 2. Evolution of the total energy obtained from the structure preserving two-fluid algorithm. In all 2×10^6 time steps, the energy deviates from its initial value by only a very small amount.

simulation using our algorithm, as seen in Fig. 3. The evolution of the perturbed electrostatic field E_z of the unstable mode is plotted in Fig. 4, which displays the space-time dependence of E_z during the nonlinear evolution of the instability.

IV. DISCUSSION AND CONCLUSION

The two-fluid scheme displayed here is very like a full-f PIC scheme for Vlasov-Maxwell systems. However, there is a difference. In full-f PIC simulations, a large number of sample points (e.g., 1000 or more sample points per grid) are needed to resolve the particle velocity distribution and reduce the numerical noise. However, in our two-fluid simulations, the effect of velocity distribution is represented by the pressure term, so particles can be very sparse (e.g., 1–4 fluid particles per grid). This significantly reduces the computation complexity as well as memory consumption.

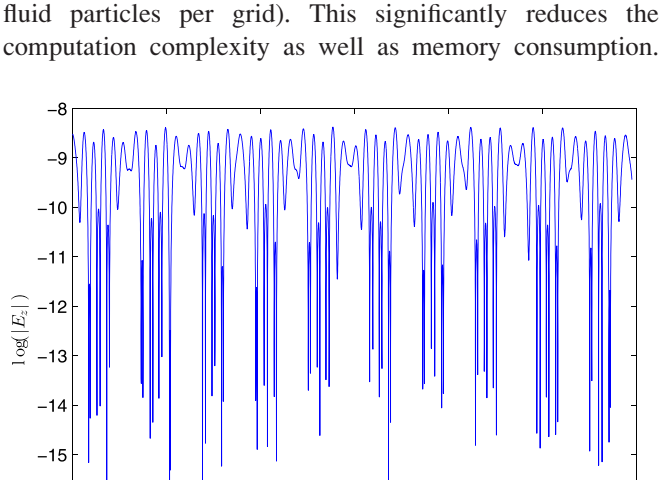

(a) Stable mode for $k_z = \pi/32$.

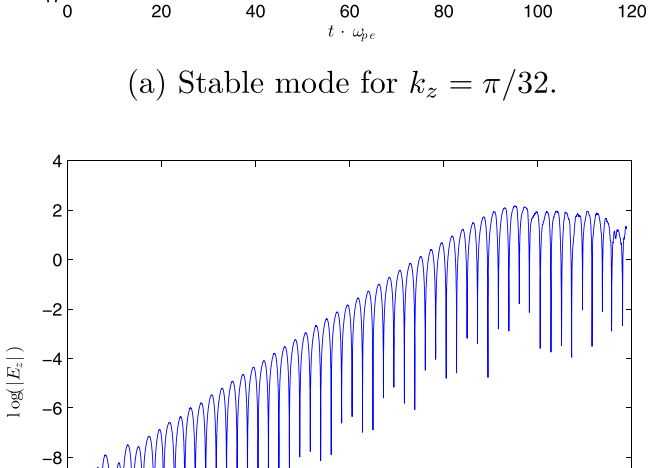

(b) Unstable mode for $k_z = \pi/128$.

FIG. 3. Simulation of the oscillating two-stream instability for an electron-positron plasma. Simulations show that the mode with $k_z = \pi/32$ is stable (a) while the $k_z = \pi/128$ is unstable (b), as predicted theoretically in Ref. 83.

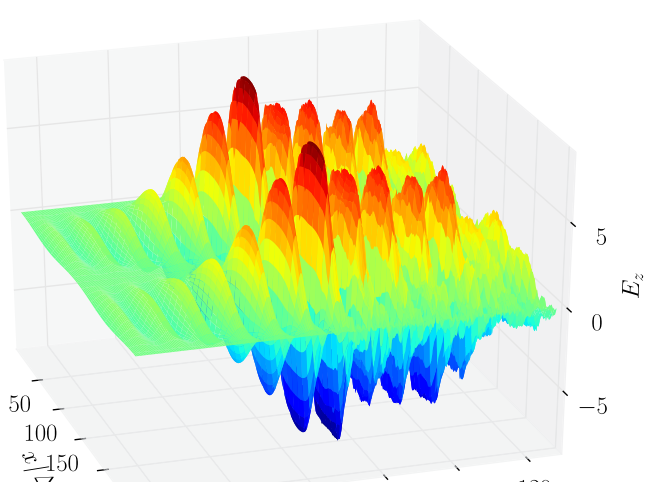

FIG. 4. The space-time dependence of E_z during the nonlinear evolution of the unstable mode initiated by a perturbation with $k_z = \pi/128$.

According to our tests, the two-fluid simulation (4 fluid particles per grid) runs about 30 times faster than a full-f PIC simulation (1000 sample points per grid) with the same parameters.

Another thing that has not been discussed yet in this paper is the boundary implement. We can state that the boundary of a particle-based scheme should be treated carefully to avoid possible numerical errors and instabilities. For structure preserving algorithms obtained from the variational theory, if the boundary is physical or the Lagrangian of the whole system is well defined, then it will be fine to obtain the scheme without introducing numerical dissipation or instabilities. For example, the Perfect Electrical Conductor boundary for electromagnetic fields and reflection for particles can be implemented in the following way. We can adopt a smaller simulation domain for particles to make sure that all smoothing functions can be evaluated on grid points inside the mesh and put a very steep potential in the boundary layer that guarantees all particles are reflected when they are near this boundary. However for absorbing boundaries, the whole system is essentially open and there is no way to guarantee conservation laws. Investigations of boundaries for this kind of problem will be a future work.

In summary, a geometric structure preserving algorithm for ideal two-fluid systems was developed. In this method, fluids were discretized as Lagrangian particles, and the conservation of mass was seen to be naturally satisfied. The electromagnetic and internal energy fields were discretized over a fixed cubic mesh using discrete differential forms. With the help of high-order Whitney interpolation forms, this scheme preserves the electromagnetic gauge symmetry. In the algorithm, the discrete pressure was obtained from the discrete internal energy field. The time integration was accomplished by adopting a powerful high-order explicit Hamiltonian splitting technique, which preserves the whole symplectic structure of the two-fluid system. Numerical examples were given to verify the accuracy and conservative nature of the geometric algorithm. We expect that this algorithm will find a wide

range of applications, especially in physical problems that are multi-scale and demand long-term accuracy and fidelity.

ACKNOWLEDGMENTS

This research was supported by ITER-China Program (2015GB111003, 2014GB124005, and 2013GB111000), JSPS-NRF-NSFC A3 Foresight Program in the field of Plasma Physics (NSFC-11261140328), the National Science Foundation of China (11575186, 11575185, 11505185, and 11505186), the Chinese Scholar Council (201506340103), the CAS Program for Interdisciplinary Collaboration Team, the Geo-Algorithmic Plasma Simulator (GAPS) project. PJM was supported by U.S. Dept. of Energy Contract No. DE-FG02-04ER-54742, and funding provided by the Alexander von Humboldt Foundation. He would also like to acknowledge the hospitality of the Numerical Plasma Physics Division of IPP, Max Planck, Garching.

[1]H. Whitney, *Geometric Integration Theory* (Princeton University Press, 1957).
[2]M. Desbrun, E. Kanso, and Y. Tong, *Discrete Differential Geometry* (Springer, 2008), pp. 287–324.
[3]J. Xiao, H. Qin, J. Liu, Y. He, R. Zhang, and Y. Sun, Phys. Plasmas (1994-present) **22**, 112504 (2015).
[4]Y. He, H. Qin, Y. Sun, J. Xiao, R. Zhang, and J. Liu, Phys. Plasmas (1994-present) **22**, 124503 (2015).
[5]P. J. Morrison, AIP Conf. Proc. **88**, 13 (1982).
[6]P. J. Morrison, Rev. Mod. Phys. **70**, 467 (1998).
[7]R. G. Spencer and A. N. Kaufman, Phys. Rev. A **25**, 2437 (1982).
[8]T. Lee, Phys. Lett. B **122**, 217 (1983).
[9]R. D. Ruth, IEEE Trans. Nucl. Sci. **30**, 2669 (1983).
[10]K. Feng, in *the Proceedings of 1984 Beijing Symposium on Differential Geometry and Differential Equations*, edited by K. Feng (Science Press, 1985), pp. 42–58.
[11]K. Feng, J. Comput. Math. **4**, 279 (1986).
[12]T. Lee, J. Stat. Phys. **46**, 843 (1987).
[13]A. P. Veselov, Funkc. Anal. Priloz. **22**, 1 (1988).
[14]H. Yoshida, Phys. Lett. A **150**, 262 (1990).
[15]E. Forest and R. D. Ruth, Phys. D **43**, 105 (1990).
[16]P. J. Channell and C. Scovel, Nonlinearity **3**, 231 (1990).
[17]J. Candy and W. Rozmus, J. Comput. Phys. **92**, 230 (1991).
[18]Y.-F. Tang, Comput. Math. Appl. **25**, 83 (1993).
[19]J. M. Sanz-Serna and M. P. Calvo, *Numerical Hamiltonian Problems* (Chapman and Hall, London, 1994).
[20]Z. Shang, Numer. Math. **83**, 477 (1999).
[21]J. E. Marsden and M. West, Acta Numer. **10**, 357 (2001).
[22]E. Hairer, C. Lubich, and G. Wanner, *Geometric Numerical Integration: Structure-Preserving Algorithms for Ordinary Differential Equations* (Springer, New York, 2002).
[23]K. Feng and M. Qin, *Symplectic Geometric Algorithms for Hamiltonian Systems* (Springer-Verlag, 2010).
[24]E. Hairer, C. Lubich, and G. Wanner, *Geometric Numerical Integration: Structure-preserving Algorithms for Ordinary Differential Equations* (Springer, 2006), Vol. 31, pp. 389–434.
[25]R. G. Littlejohn, J. Math. Phys. **20**, 2445 (1979).
[26]R. G. Littlejohn, Phys. Fluids **24**, 1730 (1981).
[27]R. G. Littlejohn, J. Plasma Phys. **29**, 111 (1983).
[28]P. J. Morrison and J. M. Greene, Phys. Rev. Lett. **45**, 790 (1980).
[29]P. J. Morrison, Phys. Lett. A **80**, 383 (1980).
[30]A. Weinstein and P. J. Morrison, Phys. Lett. A **86**, 235 (1981).
[31]J. E. Marsden and A. Weinstein, Phys. D: Nonlinear Phenom. **4**, 394 (1982).
[32]P. J. Morrison, Phys. Plasmas **20**, 012104 (2013).
[33]J. Squire, H. Qin, W. Tang, and C. Chandre, Phys. Plasmas **20**, 022501 (2013).
[34]P. J. Morrison, M. Vittot, and L. de Guillebon, Phys. Plasmas **20**, 032109 (2013).
[35]J. Burby, A. Brizard, P. Morrison, and H. Qin, Phys. Lett. A **379**, 2073 (2015).
[36]A. J. Brizard, P. J. Morrison, J. W. Burby, L. de Guillebon, and M. Vittot, "Lifting of the Vlasov-Maxwell bracket by Lie-transform method," e-print arXiv:1606.06652 (2016).
[37]H. Qin and X. Guan, Phys. Rev. Lett. **100**, 035006 (2008).
[38]H. Qin, X. Guan, and W. M. Tang, Phys. Plasmas (1994-present) **16**, 042510 (2009).
[39]X. Guan, H. Qin, and N. J. Fisch, Phys. Plasmas **17**, 092502 (2010).
[40]J. Squire, H. Qin, and W. M. Tang, Phys. Plasmas (1994-present) **19**, 052501 (2012).
[41]H. Qin, S. Zhang, J. Xiao, J. Liu, Y. Sun, and W. M. Tang, Phys. Plasmas (1994-present) **20**, 084503 (2013).
[42]J. Liu, H. Qin, N. J. Fisch, Q. Teng, and X. Wang, Phys. Plasmas **21**, 064503 (2014).
[43]R. Zhang, J. Liu, Y. Tang, H. Qin, J. Xiao, and B. Zhu, Phys. Plasmas **21**, 032504 (2014).
[44]R. Zhang, J. Liu, H. Qin, Y. Wang, Y. He, and Y. Sun, Phys. Plasmas (1994-present) **22**, 044501 (2015).
[45]C. Ellison, J. Burby, and H. Qin, J. Comput. Phys. **301**, 489 (2015).
[46]Y. He, Y. Sun, J. Liu, and H. Qin, J. Comput. Phys. **281**, 135 (2015).
[47]Y. He, Y. Sun, Z. Zhou, J. Liu, and H. Qin, preprint arXiv:1509.07794 (2015).
[48]C. L. Ellison, J. Finn, H. Qin, and W. M. Tang, Plasma Phys. Controlled Fusion **57**, 054007 (2015).
[49]J. Liu, Y. Wang, and H. Qin, preprint arXiv:1510.00780 (2015).
[50]Y. He, Y. Sun, J. Liu, and H. Qin, J. Comput. Phys. **305**, 172 (2016).
[51]J. Squire, H. Qin, and W. M. Tang, "Geometric integration of the Vlasov-Maxwell system with a variational particle-in-cell scheme," Tech. Report No. PPPL-4748, Princeton Plasma Physics Laboratory, 2012.
[52]J. Squire, H. Qin, and W. M. Tang, Phys. Plasmas (1994-present) **19**, 084501 (2012).
[53]J. Xiao, J. Liu, H. Qin, and Z. Yu, Phys. Plasmas **20**, 102517 (2013).
[54]M. Kraus, preprint arXiv:1307.5665 (2013).
[55]E. Evstatiev and B. Shadwick, J. Comput. Phys. **245**, 376 (2013).
[56]B. A. Shadwick, A. B. Stamm, and E. G. Evstatiev, Phys. Plasmas **21**, 055708 (2014).
[57]J. Xiao, J. Liu, H. Qin, Z. Yu, and N. Xiang, Phys. Plasmas (1994-present) **22**, 092305 (2015).
[58]N. Crouseilles, L. Einkemmer, and E. Faou, J. Comput. Phys. **283**, 224 (2015).
[59]H. Qin, Y. He, R. Zhang, J. Liu, J. Xiao, and Y. Wang, J. Comput. Phys. **297**, 721 (2015).
[60]H. Qin, J. Liu, J. Xiao, R. Zhang, Y. He, Y. Wang, Y. Sun, J. W. Burby, L. Ellison, and Y. Zhou, Nucl. Fusion **56**, 014001 (2016).
[61]S. D. Webb, Plasma Phys. Controlled Fusion **58**, 034007 (2016).
[62]Y. Zhou, H. Qin, J. Burby, and A. Bhattacharjee, Phys. Plasmas (1994-present) **21**, 102109 (2014).
[63]Y. Zhou, Y.-M. Huang, H. Qin, and A. Bhattacharjee, Phys. Rev. E **93**, 023205 (2016).
[64]D. Pavlov, P. Mullen, Y. Tong, E. Kanso, J. E. Marsden, and M. Desbrun, Phys. D: Nonlinear Phenom. **240**, 443 (2011).
[65]E. S. Gawlik, P. Mullen, D. Pavlov, J. E. Marsden, and M. Desbrun, Phys. D: Nonlinear Phenom. **240**, 1724 (2011).
[66]T. J. Bridges, Math. Proc. Cambridge Philos. Soc. **121**, 147 (1997).
[67]J. E. Marsden, G. W. Patrick, and S. Shkoller, Commun. Math. Phys. **199**, 351 (1998).
[68]S. Reich, J. Chem. Phys. **157**, 473 (2000).
[69]Y. J. Sun and M. Z. Qin, J. Math. Phys. **41**, 7854 (2000).
[70]T. J. Bridges and S. Reich, Phys. Lett. A **284**, 184 (2001).
[71]Y. Wang and M. Qin, J. Phys. Soc. Jpn. **70**, 653 (2001).
[72]J. Hong and M. Z. Qin, Appl. Math. Lett. **15**, 1005 (2002).
[73]J.-B. Chen, M. Qin, and Y.-F. Tang, Comput. Math. Appl. **43**, 1095 (2002).
[74]H. Y. Guo and K. Wu, J. Math. Phys. **44**, 5978 (2003).
[75]A. N. Hirani, "Discrete exterior calculus," Ph.D. thesis (California Institute of Technology, 2003).
[76]I. K. Charidakos, M. Lingam, P. Morrison, R. White, and A. Wurm, Phys. Plasmas (1994-present) **21**, 092118 (2014).
[77]J. J. Monaghan, Annu. Rev. Astron. Astrophys. **30**, 543 (1992).
[78]J. Bonet and T.-S. Lok, Comput. Meth. Appl. Mech. Eng. **180**, 97 (1999).
[79]D. J. Price and J. Monaghan, Mon. Not. R. Astron. Soc. **348**, 139 (2004).
[80]J. W. Burby and C. Tronci, "Variational approach to low-frequency kinetic-MHD in the current coupling scheme," e-print arXiv:1608.06164.
[81]K. Nishikawa, J. Phys. Soc. Jpn. **24**, 916 (1968).
[82]G. Morales, Y. Lee, and R. White, Phys. Rev. Lett. **32**, 457 (1974).
[83]H. Qin and R. C. Davidson, Phys. Plasmas (1994-present) **21**, 064505 (2014).